IOPscience iopscience.iop.org

Home Search Collections Journals About Contact us My IOPscience

Temperature-dependence of negative differential resistance in GaN/AlGaN resonant tunneling structures

This content has been downloaded from IOPscience. Please scroll down to see the full text.

2013 Semicond. Sci. Technol. 28 074024

(http://iopscience.iop.org/0268-1242/28/7/074024)

View the table of contents for this issue, or go to the journal homepage for more

Download details:

IP Address: 128.210.126.199
This content was downloaded on 06/01/2015 at 03:21

Please note that terms and conditions apply.

IOP Publishing Semiconductor Science and Technology

Semicond. Sci. Technol. 28 (2013) 074024 (5pp) doi:10.1088/0268-1242/28/7/074024

INVITED PAPER

Temperature-dependence of negative differential resistance in GaN/AlGaN resonant tunneling structures

D Li[1,2], J Shao[1,2], L Tang[1,2], C Edmunds[1], G Gardner[2,3], M J Manfra[1,2,3,4] and O Malis[1]

[1] Department of Physics, Purdue University, West Lafayette, IN 47907, USA
[2] Birck Nanotechnology Center, West Lafayette, IN 47907, USA
[3] School of Materials Engineering, Purdue University, West Lafayette, IN 47907, USA
[4] School of Electrical and Computer Engineering, Purdue University, West Lafayette, IN 47907, USA

E-mail: omalis@purdue.edu

Received 30 November 2012, in final form 8 March 2013
Published 21 June 2013
Online at stacks.iop.org/SST/28/074024

Abstract

We report a systematical study of the temperature-dependence of negative deferential resistance (NDR) from double-barrier $Al_{0.35}Ga_{0.65}N/GaN$ resonant tunneling diodes grown by plasma-assisted molecular-beam epitaxy on free-standing GaN substrates. The current–voltage (*I–V*) characterization was done in the 6–300 K temperature range. A clear NDR signature was observed for mesa sizes of $4 \times 4\ \mu m^2$ at temperatures below 130 K. This suggests that the resonant tunneling is the dominant charge transport mechanism in our devices.

(Some figures may appear in colour only in the online journal)

1. Introduction

GaN/Al(Ga)N heterostructures have attracted extensive attention in the electronics and photonics research communities in recent years. In particular, due to the large conduction band offset between GaN and AlN (1.75 eV) [1], III-nitride semiconductors have been studied for potential applications in near-infrared optoelectronic devices based on intersubband (ISB) transitions between confined states in quantum wells [2, 3]. Furthermore, due to their large longitudinal-optical phonon energies (92 meV in GaN), the nitrides are also promising candidates for high-temperature THz quantum cascade lasers (QCLs). Those applications require precise control of electron vertical transport through nitride heterostructures. Therefore, a theoretical and experimental understanding of resonant tunneling through double-barrier heterostructures and superlattices is of critical importance for design and implementation of ISB devices such as quantum well infrared photodetectors (QWIPs) and QCLs.

The double-barrier resonant tunneling diode (RTD) is the simplest device to explore quantum vertical transport. RTDs show negative deferential resistance (NDR) in the current–voltage (*I–V*) characteristics associated with resonant tunneling through quantized states in a single quantum well. This well-known phenomenon has been extensively investigated in arsenide heterostructures [4]. In all arsenide devices, it was found that the peak-to-valley ratio (PVR) increases with decreasing temperature, and that the *I–V* characteristics are exactly reproducible for the same device upon repeated measurement. Furthermore, the NDR signature is not limited to one particular direction of the sweeping bias. In contrast, resonant tunneling in nitride thin-film devices has been challenging to prove. Research on electron vertical transport in GaN/Al(Ga)N RTDs at room-temperature has been reported by several groups [5–14]. Most papers show that the NDR in c-plane RTDs appears only during the forward bias sweep of the *I–V* characteristics. In some cases the NDR disappears during backward voltage sweep while in others it disappears for subsequent forward voltage scans. These phenomena have been attributed to deep defects, which function as charge traps at interfaces. The trapped charges are supposed to lower the effective barrier height, alter the dominant transport mechanism, and eventually result in the instability of the NDR features [6, 15]. It is noteworthy

 © 2013 IOP Publishing Ltd Printed in the UK & the USA

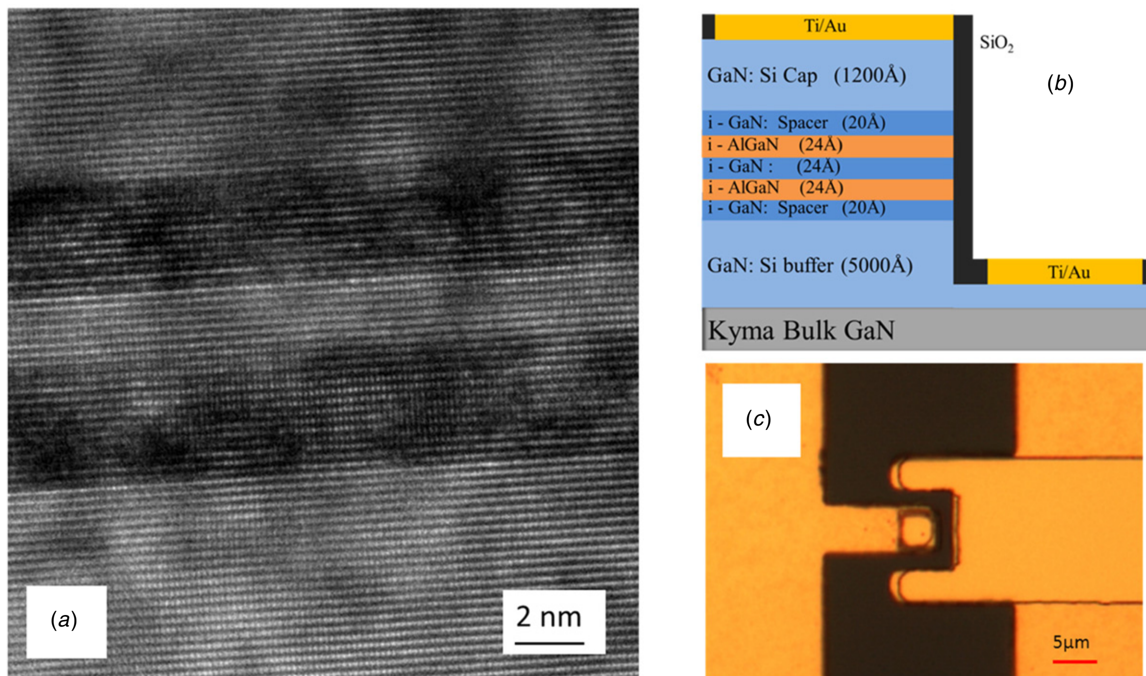

Figure 1. (*a*) TEM image of an RTD structure with the same layer thicknesses but with $Al_{0.2}Ga_{0.8}N$ barriers. (*b*) Schematic view of the layer thicknesses and doping profile of the designed RTD physical structure. (*c*) Top-view microscopy image of a fabricated $4 \times 4\ \mu m^2$ RTD device with extended top and bottom contact pads, and the mesa semi-surrounded by the bottom contact.

that NDR in nitrides has also been observed experimentally in nonpolar AlN/GaN double-barrier RTDs [11, 16] and in defect-free nanowires [17–20].

To identify the origin of NDR signatures in nitride RTDs (i.e. resonant tunneling versus charge trapping), it is necessary to examine the temperature-dependence of the *I–V* characteristics. To our knowledge, there have been relatively few reports of temperature-dependence studies of the NDR in GaN/Al(Ga)N heterostructures [21–23]. Our previous work was the first report of exactly-repeatable NDR signature in c-plane $Al_{0.2}Ga_{0.8}N$/GaN RTDs [21]. This paper focuses on the temperature-dependence of the NDR in RTDs with slightly higher Al-content in the double-barriers, i.e. GaN/$Al_{0.35}Ga_{0.65}N$ RTDs. We observe NDR at temperatures below 130 K and exactly reproducible electrical characteristics after multiple scans. Our results are consistent with theoretical expectations and measurements in other material systems, and therefore indicate that resonant tunneling is the dominant electron transport process in the devices. Our findings open the door for progress on vertical transport nitrides-based ISB devices such as THz lasers and detectors.

2. Experimental methods

The RTD structures under study were grown on free-standing c-plane GaN substrates from Kyma Technologies (dislocation density $<5 \times 10^6$ cm^{-2}) by plasma-assisted molecular-beam epitaxy (MBE) under Ga-rich conditions. Figure 1(*a*) shows the transmission electron microscopy (TEM) image of an RTD structure grown under similar conditions. The atomic force microscopy (AFM) image of the as-grown sample surface indicates a root-mean-square (RMS) roughness of 8 Å over a $10 \times 10\ \mu m^2$ region. A schematic of the layer thicknesses, doping and alloy composition of the RTD structures studied in this paper is given in figure 1(*b*). The epitaxial layers were deposited at 745 °C in a Riber 3200 MBE reactor equipped with a Veeco nitrogen plasma source. A Si-doped 500 nm thick buffer layer was deposited on the bulk substrate before growing the active layers, which also serves as bottom contact layer. The active region consists of a double-barrier *undoped* quantum well structure, $Al_{0.35}Ga_{0.65}N/GaN/Al_{0.35}Ga_{0.65}N$ with thicknesses of 24-Å/24-Å/24-Å, and is sandwiched between undoped 20 Å GaN spacers. The whole structure is capped with a 120 nm GaN layer with Si doping at a level of 1×10^{19} cm^{-3} that also serves as the top contact layer.

In order to reduce the effects of conductive dislocations, the mesa dimensions have been limited to $4 \times 4\ \mu m^2$ and the geometry of the RTD structures was designed to minimize the bottom contact resistance with the square mesa. Device fabrication was performed through standard nitride processing technology. The detailed procedure was given in [21]. A top-view microscopy image of a fabricated RTD with mesa size $4 \times 4\ \mu m^2$ is shown in figure 1(*c*).

3. Results and discussion

To measure current–voltage (*I–V*) characteristics, the semiconductor chips were mounted on copper heat sinks and wire-bonded to gold pads. The temperature-dependent *I–V* measurements were carried out from room to low temperatures in a liquid nitrogen/helium-flow cryostat. The *I–V* curves were recorded with an HP4145B semiconductor parameter analyzer that was set up to output a voltage sweep while measuring current vertically through the RTD structures. Figure 2(*a*)

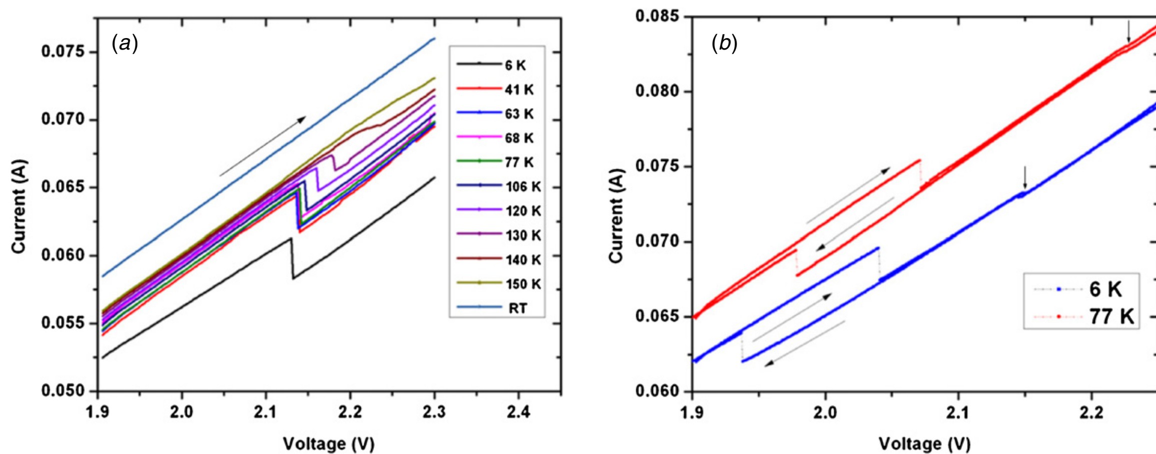

Figure 2. (*a*) Temperature-dependent *I–V* characteristics of an RTD from 6 K to room temperature (RT) by sweeping the bias on the mesa top in the same direction as indicated for all curves while recording current flowing through mesa. PVR increases as temperature decreases. (*b*) *I–V* curves from another device from the same chip with scan-up and scan-down measurement. A small feature is visible at 2.15 V (6 K) and at 2.23 V (77 K).

shows temperature-dependent *I–V* scans of a typical RTD with mesa size $4 \times 4\ \mu m^2$ during voltage sweeps from 1.9 V to 2.3 V. The clear NDR signatures were observed around 2.1 V at temperatures below 130 K. The PVR increases with decreasing temperature, in agreement with expectations. Meanwhile, the resonance shifts slightly to lower voltages as the temperature decreases, which is likely related to a drop of the series resistance in the external circuit.

Figure 2(*b*) gives the *I–V* curves of a second device (all devices from the same wafer) at 77 K and 6 K for the voltage ramp-up and ramp-down. The NDR remains clear when scanning the voltage down from high to low values, but the resonance shifts to slightly lower voltage. It is also important to note that the observed *I–V* characteristics are highly reproducible and do not diminish over multiple scans. This type of behavior (i.e. hysteresis) was not observed in lower Al-content RTDs [21], but has been reported in arsenide RTDs. The hysteresis can be attributed either to intrinsic dynamic charge built-up in the quantum well [24], or to series resistance [25, 26]. The external series resistance of our devices including measurement setup is low ($<19\ \Omega$), but due to the high leakage current (low parallel resistance), we cannot estimate the internal series resistance of the devices. Since we have not observed hysteresis in other RTD devices with $Al_{0.2}Ga_{0.8}N$ barriers [21], at this point we can only infer that the hysteretic behavior is due to an increased equivalent capacitance of the devices as compared to devices with lower-content barriers which may be related to dynamic space-charge build-up. Additional investigations are needed to elucidate the exact origin of the hysteretic behavior.

In general, the presence of NDR in *I–V* characteristics has been associated with quantum resonant tunneling transport. However, this assignment for nitride RTDs has recently been disputed in the literature [23]. Sakr *et al* observed NDR at room-temperature, but this NDR vanishes at low temperatures [23]. For this reason, they attribute the NDR features to charge trapping. In order to further investigate the vertical transport mechanism behind this phenomenon, we conducted *I–V* characteristics on RTDs as a function of temperature. In our case, the PVR of NDR increases when cooling down the device (see figures 2(*a*) and (*b*)). The lowest temperature we can reach in our current setup is 6 K, and at this temperature, we measured the highest PVR of 1.05 at a current density of 383 kA cm^{-2}. We attribute the modest value of the maximum PVR to large parallel leakage though defects, most likely threading dislocation originating from the substrates. The successive increase of the PVR with decreasing temperatures is consistent with theoretical predictions of resonant tunneling in nitrides [27] and measurements in other material systems [24].

To understand the temperature behavior of the PVR of NDR we need to consider the effect of temperature on the position of the Fermi level, carrier distribution, electron mobility and effective mass and to include the effects of electron (elastic and inelastic) scattering on tunneling [25, 28, 29]. Briefly, the temperature-dependence of the coherent tunneling is due to increased broadening of the supply function with increasing temperature that enhances the non-resonant component of the tunneling current [29]. Essentially, the PVR diminishes because the valley current increases faster with temperature than the peak current. Moreover, the temperature effect on tunneling is enhanced by inelastic scattering. Inelastic scattering, mainly phonon and interface scattering, further reduces the peak amplitude and broadens the resonant transmission probability through the double-barrier structure as compared to the coherent case. For example, Chen *et al* found that scattering-induced broadening of the resonance levels explains the dramatic decrease of the peak current in GaAs/AlGaAs RTDs [25]. In some arsenide RTDs, depending on the device structure, the NDR was found to completely disappear at high temperature [29], as we observed in our nitride devices above 150 K. In our devices, however, we also observed an overall increase of the current with increasing temperature reflected in the shift up of the *I–V* curves. This behavior can be attributed to thermionic emission and other thermally activated transport mechanisms, such as defect hopping. Therefore, the observed emergence of the NDR signature at low temperature confirms that resonant tunneling is present in our devices, and that charge trapping has no significant effect on this RTD structure.

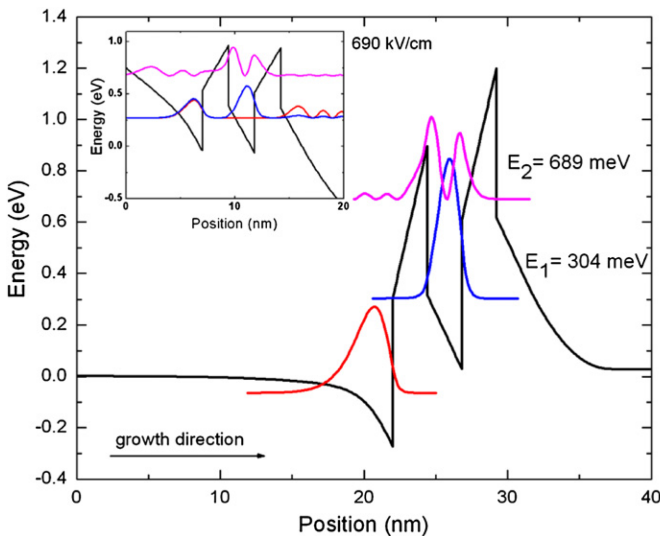

Figure 3. Schematic of the conduction band profile of the active region at zero bias from theoretical calculations. The eigenvalues of the confined states in the quantum well are $E_1 = 0.304$ eV and $E_2 = 0.689$ eV at 77 K. The inset shows the band structure under a constant applied field of 690 kV/cm.

The schematic of the conduction band profile (at the Γ point) in the active region of our designed RTD structure at zero bias is given in figure 3. The calculations were performed with the self-consistent Schrödinger–Poisson solver *nextnano3* [30]. The asymmetry of the conduction band is due to the strong polarization discontinuity of the spontaneous and piezoelectric fields at the interfaces between GaN and AlGaN. The polarization field also results in quantized levels at the first heterointerface on the left. Therefore, resonant tunneling is expected to occur between the lowest level in the triangular well (red curve with energy $E = -0.063$ eV in figure 3) and the quantized levels of the QW (E_1 and E_2), as indicated in the inset of figure 3. The designed structure exhibits two confined states at $E_1 = 0.304$ eV and $E_2 = 0.689$ eV, respectively. The calculated conduction band offset between GaN and $Al_{0.35}Ga_{0.65}N$ is about 0.58 eV. Note that there are two quantized energy states in the theoretical simulations, while in our measurements there is only one clear NDR signature. Nevertheless, a second feature can be observed in figure 2(*b*) at 2.15 V (6 K) and at 2.23 V (77 K) (indicated with arrows in figure 2(*b*)), which may be related to tunneling through the first excited state of the quantum well. The absence of a strong second NDR signature is most likely due to a weak confinement of the higher energy state (E_2) since the barrier height of the confinement layers becomes lower when forward bias is applied. In order to observe two clear NDRs from RTDs, it is necessary to increase the Al-composition in the barriers. Higher Al composition in barriers would also enable room temperature operation of the devices. However, this is relatively challenging from a material growth standpoint because in order to observe NDR it is also crucial to maintain smooth interfaces and to minimize defect formation in higher Al layers and at heterointerfaces [9, 11].

4. Conclusions

In summary, we conducted an investigation of the temperature-dependence of NDR from a double-barrier $Al_{0.35}Ga_{0.65}N/GaN$ RTD grown by MBE on free-standing GaN templates. A clear NDR signature has been obtained at various temperatures for a small size device with an area of $4 \times 4\ \mu m^2$. We note that no NDR was observed from larger size devices (from $6 \times 6\ \mu m^2$ to $30 \times 30\ \mu m^2$). The explanation of the observations lies in the current leakage through screw dislocations. Since the number of the conductive dislocations is proportional to the area of the mesa, the increase of leakage current with the device area eventually obscures the NDR. Considering all facts from our results and from literature, we conclude that the material quality is most critical for success of the nitride RTDs. We expect that a practical nitride-based RTD operating at room temperature will be developed in the near future if the material quality can be significantly improved. The material optimization includes constant enhancement of epilayer growth, optimization of polarization balance and device structure (layer thickness and doping concentration), and defect reduction in the substrate and epilayers. Our results are a promising step toward successful development of the nitride's high-speed infrared lasers and detectors.

Acknowledgments

This work was supported by the NSF award nos. ECCS-1001431, DMR-1206919 and ECCS-1253720, and from the Defense Advanced Research Project Agency (DARPA) under contract no. D11PC20027.

References

[1] Tchernycheva M, Nevou L, Doyenette L, Julien F H, Warde E, Guillot F, Monroy E, Bellet-Amalric E, Remmele T and Albrecht M 2006 Systematic experimental and theoretical investigation of intersubband absorption in GaN/AlN quantum wells *Phys. Rev. B.* **73** 125347

[2] Suzuki N and Iizuka N 1997 Feasibility study on ultrafast nonlinear optical properties of 1.55-μm intersubband transition in AlGaN/GaN quantum wells *Japan. J. Appl. Phys.* **36** L1006–8

[3] Iizuka N, Kaneko K and Suzuki N 2002 Near-infrared intersubband absorption in GaN/AlN quantum wells grown by molecular beam epitaxy *Appl. Phys. Lett* **81** 1803–5

[4] Gering J M 1991 *The Characterization of Aluminum Gallium Arsenide Resonant Tunneling Diodes at Microwave Frequencies* (Champaign, IL: University of Illinois Press)

[5] Mietze C, Lischka K and As D J 2012 Current–voltage characteristics of cubic Al(Ga)N/GaN double barrier structures on 3C–SiC *Phys. Status Solidi A* **209** 439–42

[6] Golka S, Pflugl C, Schrenk W, Strasser G, Skierbiszewski C, Siekacz M, Grzegory I and Porowski S 2006 Negative differential resistance in dislocation-free GaN/AlGaN double-barrier diodes grown on bulk GaN *Appl. Phys. Lett.* **88** 172106

[7] Baumann E, Giorgetta F R, Hofstetter D, Wu H, Schaff W J, Eastman L F and Kirste L 2005 Tunneling effects and intersubband absorption in AlN/GaN superlattices *Appl. Phys. Lett.* **86** 032110

[8] Belyaev A E, Foxon C T, Novikov S V, Makarovsky O, Eaves L, Kappers M J and Humphreys C J 2003 Comment

on 'AlN/GaN double-barrier resonant tunneling diodes grown by rf-plasma-assisted molecular-beam epitaxy' *Appl. Phys. Lett.* **83** 3626–7 [Appl. Phys. Lett. 81, 1729 (2002)]

[9] Bayram C, Vashaei Z and Razeghi M 2010 Room temperature negative differential resistance characteristics of polar III-nitride resonant tunneling diodes *Appl. Phys. Lett.* **96** 042103

[10] Vashaei Z, Bayram C and Razeghi M 2010 Demonstration of negative differential resistance in GaN/AlN resonant tunneling diodes at room temperature *J. Appl. Phys.* **107** 083505

[11] Bayram C, Vashaei Z and Razeghi M 2010 Reliability in room-temperature negative differential resistance characteristics of low-aluminum content AlGaN/GaN double-barrier resonant tunneling diodes *Appl. Phys. Lett* **97** 181109

[12] Boucherit M, Soltani A, Monroy E, Rousseau M, Deresmes D, Berthe M, Durand C and De Jaeger J-C 2011 Investigation of the negative differential resistance reproducibility in AlN/GaN double-barrier resonant tunnelling diodes *Appl. Phys. Lett.* **99** 182109

[13] Sakr S, Kotsar Y, Tchernycheva M, Warde E, Isac N, Monroy E and Julien F H 2012 Resonant tunneling transport in a GaN/AlN multiple-quantum-well structure *Appl. Phys. Express* **5** 052203

[14] Kikuchi A, Bannai R, Kichino K, Lee C M and Chyi J-I 2002 AlN/GaN double-barrier resonant tunneling diodes grown by rf-plasma-assisted molecular-beam epitaxy *Appl. Phys. Lett.* **81** 1729–31

[15] Yang L, He H, Mao W and Hao Y 2011 Quantitative analysis of the trapping effect on terahertz AlGaN/GaN resonant tunneling diode *Appl. Phys. Lett.* **99** 153501

[16] Zainal N, Novikov S V, Mellor C J, Foxon C T and Kent A J 2010 Current-voltage characteristics of zinc-blende (cubic) $Al_{0.3}Ga_{0.7}N$/GaN double barrier resonant tunneling diodes *Appl. Phys. Lett.* **97** 112102

[17] Songmuang R, Katsaros G, Monroy E, Spathis P, Bougeral C, Mongillo M and De Franceschi S 2010 Quantum transport in GaN/AlN double-barrier heterostructure nanowires *Nano Lett.* **10** 3545–50

[18] Rigutti L, Jacopin G, De Luna Bugallo A, Tchernycheva M, Warde E, Julien F H, Songmuang R, Galopin E, Largeau L and Armand J-C 2010 Investigation of the electronic transport in GaN nanowires containing GaN/AlN quantum discs *Nanotechnology* **21** 425206

[19] Li E, Zhu P, Zhao T, Ma D and Wang X 2012 Study of electronic structures and transport properties on saturated GaN nanowires *Adv. Mater. Res.* **465** 118–24

[20] Carnevale S D, Marginean C, Phillips P J, Kent T F, Sarwar A T M G, Mills M J and Myers R C 2012 Coaxial nanowire resonant tunneling diodes from non-polar AlN/GaN on silicon *Appl. Phys. Lett.* **100** 142115

[21] Li D, Tang L, Edmunds C, Shao J, Gardner G, Manfra M J and Malis O 2012 Repeatable low-temperature negative-differential resistance from $Al_{0.18}Ga_{0.82}N$/GaN resonant tunneling diodes grown by molecular-beam epitaxy on free-standing GaN substrates *Appl. Phys. Lett.* **100** 252105

[22] Foxon C T *et al* 2003 Current–voltage instabilities in GaN/AlGaN resonant tunnelling structures *Phys. Status Solidi C* **0** 2389–92

[23] Sakr S, Warde E, Tchernycheva M, Rigutti L, Isac N and Julien F H 2011 Origin of the electrical instabilities in GaN/AlGaN double-barrier structure *Appl. Phys. Lett.* **99** 142103

[24] Goodings C J, Mizuta H and Cleaver J R A 1994 Electrical studies of charge built-up and phonon-assisted tunneling in double-barrier materials with very thick spacer layers *J. Appl. Phys.* **75** 2291–3

[25] Chen J, Chen J G, Yang C H and Wilson R A 1991 The *I-V* characteristics of double-barrier resonant tunneling diodes: observation and calculation on their temperature dependence and asymmetry *J. Appl. Phys.* **70** 3131–6

[26] Hou Y, Wang W-P, Li N, Wu W and Fu Y 2008 Effects of series and parallel resistances on current-voltage characteristics of small-area air-bridge resonant tunneling diode *J. Appl. Phys.* **104** 074508

[27] Sakr S, Warde E, Tchernycheva M and Julien F H 2011 Ballistic transport in GaN/AlGaN resonant tunneling diodes 2011 *J. Appl. Phys.* **109** 023717

[28] Shen G D, Xu D X, Willander M and Hansson G V 1991 The origin of the temperature dependence in resonant tunneling transport *Proc. IEEE/Cornell Conf. on Advanced Concepts in high Speed Semiconductor Devices and Circuits* pp 84–93

[29] Vanbesien O, Bouregba R, Mounaix P and Lippens D 1991 Temperature dependence of peak to valley ratio in resonant tunneling double barriers *Resonant Tunneling in Semiconductors* ed L L Chang *et al* (NATO ASI Series B, vol 277) (New York: Plenum)

[30] Birner S, Zibold T, Andlauer T, Kubis T, Sabathil M, Trellakis A and Vogl P 2007 Nextnano: general purpose 3D simulations *IEEE Trans. Electron Devices* (The nextnano software can be obtained from http://www.nextnano.de and http://www.wsi.tum.de/nextnano) **54** 2137–42